Angewandte Chemie
Eine Zeitschrift der Gesellschaft Deutscher Chemiker

Supporting Information

Phase Separation of Oppositely Charged Polymers Regulates Bioinspired Silicification

*H. Zhai, T. Bendikov, A. Gal**

SUPPORTING INFORMATION

Table of contents

SUPPORTING INFORMATION

Experimental Section

Reagents. Sodium silicate solution ($(NaOH)_x(Na_2SiO_3)_y \cdot zH_2O$, 27% SiO_2, ~6 M) from Sigma-Aldrich was used as the silicon source. Polyelectrolytes including poly(allylamine hydrochloride) (average M_w ~ 50 kDa, PAH^+/Cl^- = 1), branched polyethyleneimine (M_w ~ 750 kDa), and poly(acrylic acid, sodium salt) (M_w ~ 15 kDa, PAA^-/Na^+ = 1) were purchased from Sigma-Aldrich and used without any further treatment. The reported polymer concentrations are the concentration of the functional groups, which were calculated using the reported polymer purities and average sizes. Milli-Q water (resistivity: 18.2 MΩ·cm at 25 ℃) was used for solution preparation. To synthesize silica under mild conditions, all experiments were carried out at pH 5.0 (adjusted with 1 M HCl/NaOH) at room temperature.

Precipitation experiments. Precipitation experiments were conducted according to the schemes shown in Figure 2a. A 25 µL of 200 mM PAH stock solution was dilute in milli-Q water (Sequence I), Si (Sequence II), and NaCl solutions (Sequence III), respectively. Subsequently, a 25 µL of 200 mM PAA stock solution was added for phase separation. For Sequences I and III, after phase separation, freshly prepared Si solutions (200 mM) were added to reach target concentrations for silicification. The final volumes of all reaction systems were 1 mL. Precipitation experiments for PAH + phosphate, PEI + PAA, and PEI + phosphate pairs followed Sequence III for adjusting ionic strength. To achieve low ionic strength conditions for PEI + PAA pairs, the stock solutions were dialyzed for 4 h. The concentrations of the components under each experimental reaction in Figure 6 are shown in Table S3 and S4.

DLS. Dynamic light scattering instrument (Zetasizer Nano ZSP, Malvern Instruments, United Kingdom) equipped with a 633 nm laser was used to measure particle sizes in real-time. Raw correlograms are shown in Figure S2. A correlation coefficient value of 0.3 was used as a threshold to report the presence of particles in the solution. The particle sizes were determined by intensity distribution and presented as the average values of three replicate measurements.

PHREEQC simulations. PHREEQC Interactive Version 3.3.7.11094 was used to model Si solutions with the wateq4f database. The simulations were performed in two steps: in the first step, the initial solution is equilibrated to calculate the $Si(OH)_4$ activities and the equilibrated solution was allowed to calculate the saturation indices with respect to possible Si-phases.

SEM observation of precipitate samples. Samples were centrifuged at 14000 g for 5 min. The pellets were washed with Milli-Q water three times to remove unreacted phases. Washed pellets were lyophilized and mounted onto SEM holders. The samples were coated with 5 nm iridium (Compact Coating Unit, CCU-010, Safematic), and imaged using SEM (Sigma, Zeiss).

XPS analysis. The surface components of the lyophilized silica precipitates were detected by X-ray photoelectron spectroscopy (XPS) under ultra-high vacuum conditions (5×10^{-10} Torr) using Kratos AXIS ULTRA system with a monochromatic Al Ka X-ray source ($h\nu$ = 1486.6 eV) at 75W with a detection pass energy of 20-80 eV. A low-energy electron flood gun (eFG) was applied for charge neutralization. To define binding energies (BE) of different elements, the C 1s peak at 284.8 eV was taken as a reference. Curve fitting analysis was based on linear or Shirley background subtraction and application of Gaussian-Lorenzian line shapes.

SUPPORTING INFORMATION

Quantification of precipitated Si. The amount of precipitated silica was determined using commercial silica test kit. The washed pellet was dissolved in 50 µL of 2 M NaOH by incubation at 95 ℃ for 1 h. The reacted solution was further diluted to 5 mL using milli-Q water and the silica concentration was subsequently determined using the silicate test kit (Merck Millipore, USA). The amount of silica was calculated by measured Si-concentration × 5 mL and present as the average values of three replicate measurements.

TGA. Lyophilized samples from several batches were collected for bulk components analyses. The precipitates were analyzed by thermal gravimetric analysis (SDT Q600, TA Instruments, USA). Analyses were performed under air atmosphere (injection rate of 100 mL/min) with a heating rate of 10 K/min. To calculate initial Si content, we assume the ratio of PAH to PAA is 1:1. When Si is present as $Si(OH)_4$, the molecular ratios of Si to PAH + PAA become ~0.1 (low Si) and ~1.3 (high Si) which are very close to the Si/ (PAH + PAA) ratios obtained by XPS measurements.

***In situ* observation using cryo-TEM.** 3 µL sample solution was dropped on the carbon side of plasma-discharged cleaned holey carbon R 0.6/1 Cu 200 mesh grids (Quantifoil). The back-blotted grid was vitrified using a Leica EM GP automatic plunger (Leica, Vienna, Austria) under 25 °C and 90% humidity conditions. Vitrified specimens were kept in liquid nitrogen until being used. Cryo-TEM imaging was performed on a FEI Tecnai T12 TEM microscope (Thermo Fisher Scientific, USA) equipped with an XF416 TVIP camera (TVIPS GmbH, Germany) and Gatan cryo-holders (Gatan 626-60/70, Gatan inc, USA). Images were recorded under low-dose mode with an accelerating voltage of 120 kV. For preparing dry TEM samples, a drop of 5 µL sample was deposited on a plasma-discharged carbon film grid (CF200-Cu) and then the water was blotted off with filter paper. The FEI Spirit TEM microscope equipped with a bottom-mount CCD camera (FEI Eagle 2k × 2k) was used to image dry samples with the accelerating voltage of 120 kV.

SUPPORTING INFORMATION

Table S1. PHREEQC simulating saturation indices with respect to various possible SiO_2-phases in $Si(OH)_4$ solutions at pH 5.0, 25 ℃.

$[Si(OH)_4]$	Activity (mM)			Saturation indices		
(mM)	$Si(OH)_4$	$Si(OH)_3O^-$	$Si(OH)_2O_2^{2-}$	Quartz	SiO_2 gel	Amorphous SiO_2
10	10	1.62×10^{-4}	1.42×10^{-12}	1.98	1.02	0.71
100	100	1.92×10^{-3}	2.46×10^{-11}	3.00	2.03	1.73

Table S2. XPS elemental analyses of silica-precipitates induced by PAH-PAA polymer-dense phases.

Sample No.	Reaction Sequence	Atomic concentrations (%)					
		C	O	N	Si	Cl	Na
2	PAH→PAA→Si (low)	63.35 ± 4.71	25.21 ± 3.11	7.59 ± 0.94	3.35 ± 2.54	0.31 ± 0.08	0.04 ± 0.08
3	PAH→PAA→Si (high)	49.21 ± 2.90	33.94 ± 3.20	8.35 ± 0.63	6.78 ± 0.81	1.45 ± 0.49	0.09 ± 0.10
4	PAH→Si (low) →PAA	63.32 ± 1.25	24.16 ± 1.26	8.79 ± 0.22	1.87 ± 0.55	1.07 ± 0.14	0.67 ± 0.13
5	PAH→Si (high) →PAA	35.58 ± 2.43	44.45 ± 2.55	4.99 ± 0.58	13.27 ± 1.97	1.00 ± 0.10	0.58 ± 0.12
7	PAH→NaCl (high)→PAA→Si (high)	33.05 ± 1.57	46.84 ± 1.56	4.14 ± 0.30	14.63 ± 1.50	0.67 ± 0.12	0.56 ± 0.15
11	PAH→NaCl (low)→PAA→Si (low)	63.88 ± 1.84	24.16 ± 1.78	7.76 ± 0.34	2.01 ± 0.26	1.22 ± 0.15	0.85 ± 0.18

Table S3. Nominal molar concentrations (in mM) of the components for experimental reaction described in Figure 6 at low ionic strength level.

Samples		Solution components (mM)				
		[polycation]	[polyanion]	$[Si(OH)_4]$	$[Na^+]$	$[Cl^-]$
PAH+P	without Si	10	30	0	32	10
	with Si	10	30	100	109.5	82.4
PEI+PAA	without Si	5	5	0	0.05	0.04
	with Si	5	5	100	77.6	72.4
PEI+P	without Si	10	30	0	30.6	8.6
	with Si	10	30	100	108.1	81

Table S4. Nominal molar concentrations (in mM) of the components for experimental reaction described in Figure 6 at high ionic strength level.

Samples		Solution components (mM)				
		[polycation]	[polyanion]	$[Si(OH)_4]$	$[Na^+]$	$[Cl^-]$
PAH+P	without Si	10	30	0	182	160
	with Si	10	30	100	259.5	232.4
PEI+PAA	without Si	5	5	0	5	4.8
	with Si	5	5	100	82.5	77.2
PEI+P	without Si	10	30	0	180.6	158.6
	with Si	10	30	100	258.1	231

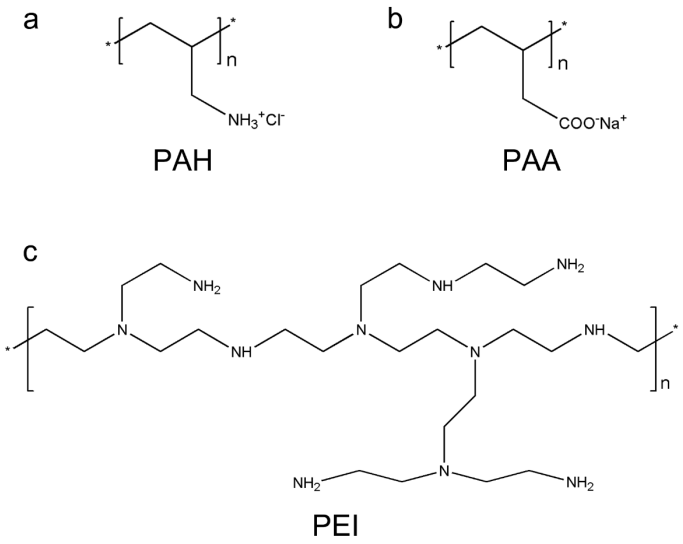

Figure S1. Molecular structures of polymers used in the present research.

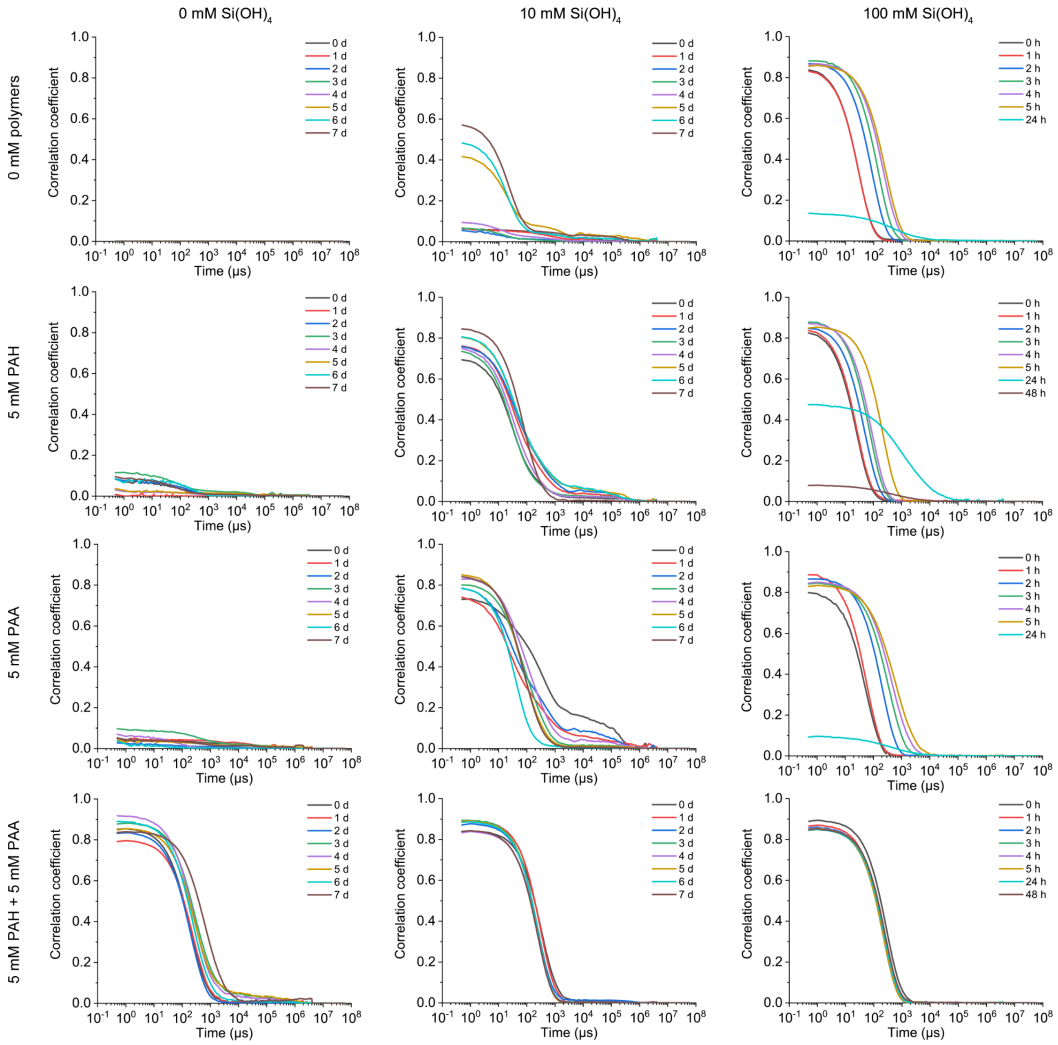

Figure S2. Raw DLS correlograms for soluble silica solutions with increasing [$Si(OH)_4$] concentrations (0 mM (left), 10 mM (middle), 100 mM (right)) and added polymers (no polymers (top), 5 mM PAH (second from the top), 5 mM PAA (second from the bottom) and 5mM PAH + 5 mM PAA (bottom)) measured at different time points. Each measurement consists of three replicates. The correlation coefficient increases with time in the 10 mM $Si(OH)_4$ due to the formation of silica colloids, while in the 100 mM $Si(OH)_4$ eventual decrease represents silica-gelation.

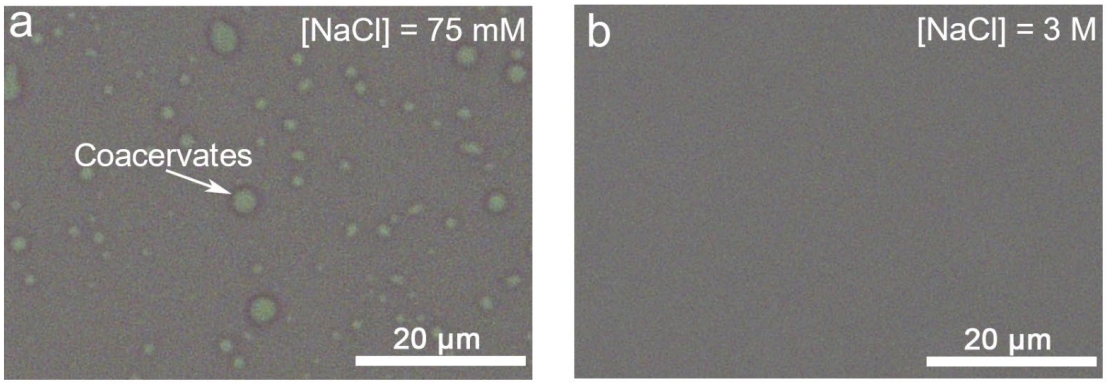

Figure S3. Optical microscopy images of coacervates forming in 5 mM PAH and 5 mM PAA with (a) 75 mM, and (b) 3 M NaCl, showing that ultrahigh concentration of NaCl inhibits PAH-PAA coacervation. White arrow in (a) highlights PAH-PAA coacervates.

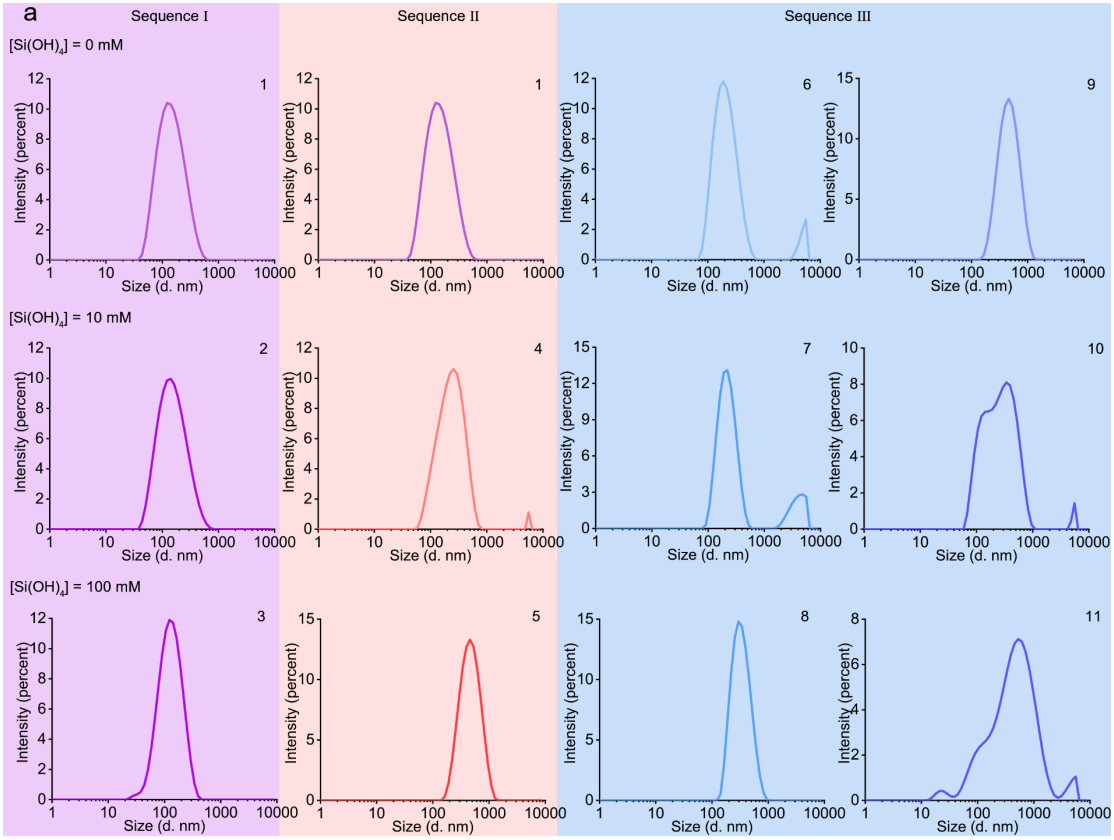

b

No.	Samples	Solution components (mM)				
		[PAH]	[PAA]	[$Si(OH)_4$]	[Na^+]	[Cl^-]
1	PAH→PAA	5	5	0	5.7	5.4
2	PAH→PAA→Si (low)	5	5	10	13.5	11.7
3	PAH→PAA→Si (high)	5	5	100	83.2	77.8
4	PAH→Si (low)→PAA	5	5	10	13.5	11.7
5	PAH→Si (high)→PAA	5	5	100	83.2	77.8
6	PAH→NaCl (low)→PAA	5	5	0	13.2	12.9
7	PAH→NaCl (low)→PAA→Si (low)	5	5	10	21.0	19.2
8	PAH→NaCl (low)→PAA→Si (high)	5	5	100	90.7	85.3
9	PAH→NaCl (high)→PAA	5	5	0	80.7	80.4
10	PAH→NaCl (high)→PAA→Si (low)	5	5	10	88.5	86.7
11	PAH→NaCl (high)→PAA→Si (high)	5	5	100	157.9	152.8

(pH 5.0, 25 °C, σ[Si (low)] = 0.71, σ[Si (high)] = 1.73)

Figure S4. Particle sizes measured by DLS. (a) Particle size distributions under different conditions labeled by numbers in the top right corners of each diagram and described in (b). These results are in agreement with the cryo-TEM observations (Figure 4).

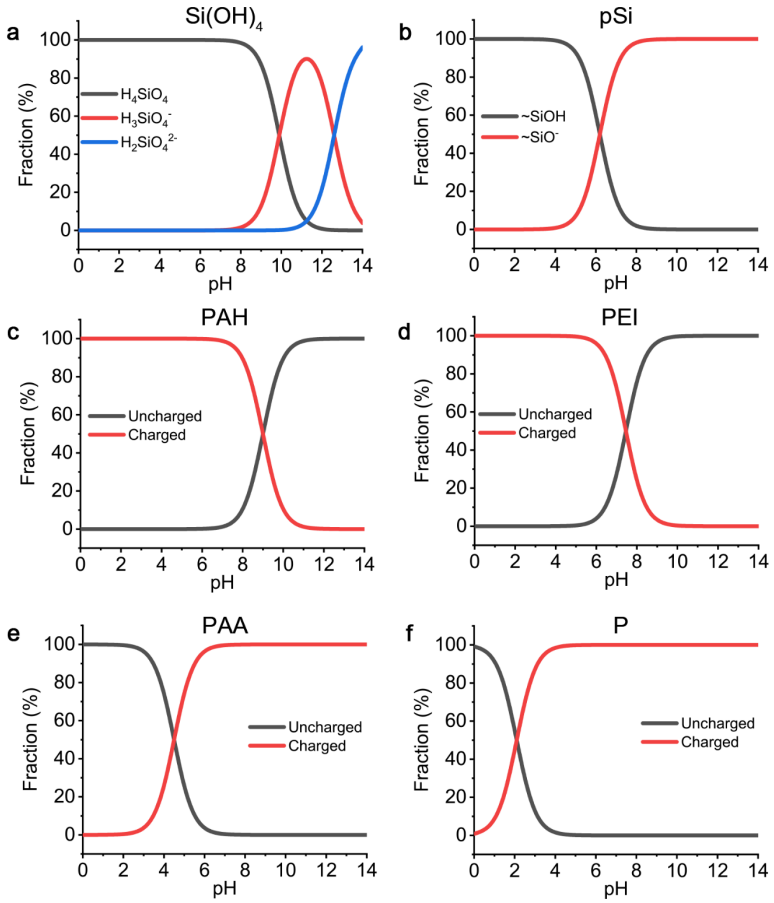

Figure S5. The relative speciation distributions of (a) mono silicic acid ($Si(OH)_4$), (b) poly silicic acid (pSi), (c) PAH, (d) PEI, (e) PAA and (f) phosphate (P). The components were calculated based on pKa values of 9.9, 6.8, 8.9, 7.5, 4.5, and 2.1 for $Si(OH)_4$, pSi, PAH, PEI, PAA, and P, respectively.[1–5]

References

[1] A. C. Makrides, M. Turner, J. Slaughter, *J. Colloid Interface Sci.* **1980**, *73*, 345–367.

[2] V. V. Annenkov, E. N. Danilovtseva, V. A. Pal'shin, O. N. Verkhozina, S. N. Zelinskiy, U. M. Krishnan, *RSC Adv.* **2017**, *7*, 20995–21027.

[3] S. Kobayashi, *Macromolecules* **1987**, 1496–1500.

[4] K. A. Curtis, D. Miller, P. Millard, S. Basu, F. Horkay, P. L. Chandran, *PLoS One* **2016**, *11*, 1–20.

[5] B. N. Dickhaus, R. Priefer, *Colloids Surfaces A* **2016**, *488*, 15–19.